International Journal Of Innovative Trends In Multi Disciplinary Scientific Research
ISSN (Online): 3139 – 2687
(www.ijtmsr.co.in) Volume 9, Issue 6, 2026

Design Optimization, Fabrication, and Structural-Modal Analysis of a 3D-Printed Industrial Robotic Arm Using Aluminium and Composite Materials

Malla Surendra[1], G. Sunil[2]

[1]PG scholar, Department of Mechanical engineering, Visakha Institute of Engineering & Technology (A), Narava, Visakhapatnam, Andhra Pradesh, India
[2]Assistant professor, Department of Mechanical engineering, Visakha Institute of Engineering & Technology (A), Narava, Visakhapatnam, Andhra Pradesh, India

Abstract

This paper presents a comprehensive computational design, optimization, and structural-modal analysis of a lightweight material-handling industrial robotic arm, referred to as the Smokie robot, intended for logistics operations with a maximum payload capacity of 30 kg. Two structural configurations (Model 1 and Model 2) were generated in CATIA and evaluated using Finite Element Analysis (FEA) in ANSYS across four candidate materials—Aluminium, Carbon Fibre Reinforced Polymer (CFRP), E-Glass Fibre Reinforced Polymer (E-GFRP), and S-Glass Fibre Reinforced Polymer (S-GFRP). Static structural analysis, modal analysis, and harmonic vibration analysis were performed to evaluate deformation, von Mises stress, strain, natural frequency, and dynamic amplitude response. Results indicate that although Aluminium exhibits comparatively higher mass, it consistently produces the lowest deformation, stress, and strain across all links while remaining within allowable limits, establishing it as the structurally optimum material. Between the two structural configurations, Model 2 offers reduced mass at the cost of marginally higher deformation and stress, both remaining within safe design limits, and is therefore identified as the preferred geometric configuration. The study provides a methodological framework for balancing weight optimization against structural reliability in the design of logistics-handling robotic manipulators.

Keywords: Robotic arm; Finite Element Analysis; CATIA; ANSYS; structural analysis; modal analysis; harmonic analysis; aluminium; CFRP; GFRP; material optimization; logistics automation.

I. INTRODUCTION

Material-handling robots have become central to modern logistics operations, automating the movement, storage, and protection of goods across the supply chain. The integration of machine learning, computer vision, and artificial intelligence has extended robotic capability to complex picking, packing, palletizing, and shipping tasks that were traditionally performed manually, reducing labour costs and minimizing human error [1]-[3]. Beyond throughput gains, robotic material handling improves workplace safety by removing human operators from repetitive or hazardous lifting tasks.

The present work investigates "Smokie," a six-link articulated logistics robot designed to handle payloads up to 30 kg. As a collaborative robot (cobot), Smokie is intended to operate safely alongside human workers while performing repetitive lifting and transport duties. Its structural design must simultaneously satisfy competing requirements of minimum weight, for energy efficiency and dynamic responsiveness, and sufficient stiffness and strength, to avoid excessive deflection or failure under load.

Robot frame construction commonly employs aluminium or steel for their strength-to-weight characteristics, while fibre-reinforced polymer composites (CFRP, E-GFRP, S-GFRP) are increasingly adopted where higher specific stiffness and fatigue resistance are required. This study systematically compares these four candidate materials across two alternative link geometries using Finite Element Analysis (FEA), evaluating structural, modal, and

harmonic performance to identify the optimum material-geometry combination for the Smokie robot structure.

A. Aim and Objectives

The aim of this work is to develop a lightweight yet structurally robust robotic arm optimized for 30 kg payload logistics handling. The specific objectives are: (i) to evaluate Aluminium, CFRP, E-GFRP, and S-GFRP for their suitability in balancing weight, strength, and durability; (ii) to perform FEA-based structural analysis of two link-geometry configurations under static loading; (iii) to conduct modal and harmonic vibration analysis to characterize dynamic behaviour and identify resonance risk; and (iv) to recommend an optimum material-model combination for practical implementation.

II. LITERATURE REVIEW

Prior work on articulated manipulators has predominantly addressed kinematic and dynamic modelling. Yazdanpanah derived geometric Jacobians and identified kinematic singularities for 6-DOF arms including the Barrett WAM and Smokie OUR robot [1]. Hansen et al. proposed a non-iterative algorithm for workspace generation of general n-R manipulators [2]. Mir-Nasiri introduced a parallel-structure robotic arm design offering advantages over conventional SCARA manipulators [3], while Park et al. presented kinematic and dynamic analysis of a dual-arm mobile platform for electrical device assembly [4]. Schilling detailed Denavit-Hartenberg based design and control methodology applicable to general robotic manipulators [5], and related studies developed forward/inverse kinematic models for multi-DOF arms used in pick-and-place and welding applications [6]-[10].

Regarding materials, several studies emphasize composite reinforcement as a route to lightweight, high-stiffness robotic structures. Lee et al. demonstrated that fibre-reinforced composites offer superior strength-to-weight and modulus-to-weight ratios relative to conventional metals for robotic structures [14]. Related studies on biped robot foot structures and lightweight serial mechanisms confirm that composite epoxy materials provide higher specific fatigue limits and improved damping compared to aluminium [15]-[16]. Investigations into natural-fibre composites note that, despite their sustainability advantages, they remain outperformed by CFRP and GFRP in strength-critical robotic applications [17], [19]. Additional studies address deflection reduction in flexible composite manipulators through structural and dynamic modelling [20]-[21]. Collectively, the literature establishes both the kinematic design foundations and the material-selection rationale motivating the present comparative FEA study.

III. DESIGN PARAMETERS

The robot structure was designed for a maximum payload of 30 kg with a workspace diameter of 1.9 m and a range of motion of 0°-180°. The base is secured using 12 mm bolts to distribute load evenly, and the arm comprises six links with five degrees of freedom, actuated through motors in a parallel configuration. Each link was modelled as a hollow pipe section of 4 mm wall thickness to minimize mass while preserving load-carrying capacity. Two structural configurations, Model 1 and Model 2, were developed to compare geometric influence on structural response, and four candidate materials were evaluated for each configuration.

IV. METHODOLOGY

A. CAD Modelling

The geometry of each of the six links (Fig. not reproduced) was developed in CATIA V5 using the Pad and Pocket features under the Part Design workbench. Link 1, the base component, has an outer diameter of 75 mm, wall thickness of 4 mm, and a mounting flange of 167 mm diameter. Links 2-5 maintain the same 75 mm outer diameter and 4 mm wall thickness with lengths of 110 mm, 430 mm, 436 mm, and 109 mm respectively, while Link 6 forms a two-fingered end effector for gripping payloads. Component assembly was performed using the Offset and Coincidence constraints in the Assembly Design workbench, with careful verification to eliminate part interference prior to export.

B. Finite Element Analysis Setup

The verified CATIA assemblies were imported into ANSYS Workbench via STEP files for Finite Element Analysis. Geometry was discretized using tetrahedral elements with a global mesh size of 4 mm, yielding a representative mesh of 15,512 elements and 22,758 nodes. Boundary conditions fixed the base mounting plate, while a 300 N force (representing the 30 kg design payload) was applied at the end effector along the Z-

International Journal Of Innovative Trends In Multi Disciplinary Scientific Research
ISSN (Online): 3139 – 2687
(www.ijtmsr.co.in) Volume 9, Issue 6, 2026

direction, together with standard earth gravity (9806.6 mm/s²) to account for self-weight. Static structural, modal, and harmonic response analyses were performed for each of the four material assignments—Aluminium, CFRP, E-GFRP, and S-GFRP—using their respective Young's modulus, Poisson's ratio, and density values.

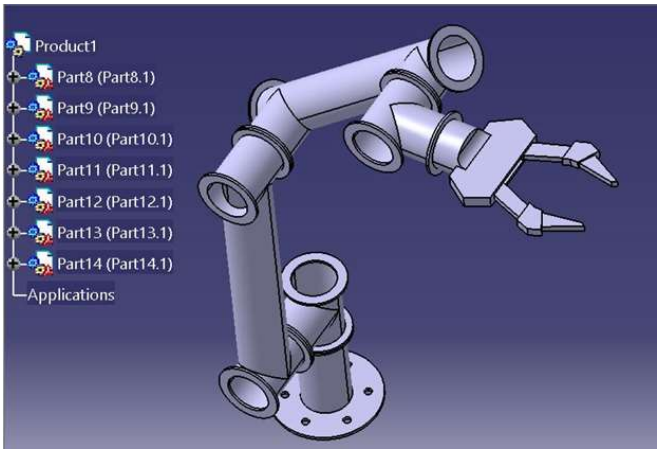


Fig 1: assembly of model 1.

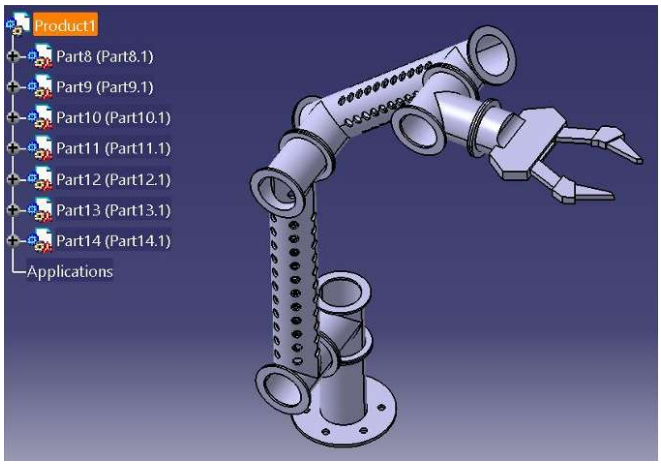


Fig 2: assembly of model 2.

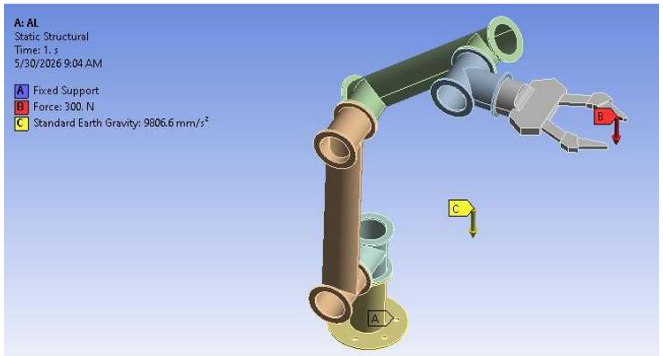


Fig 3: Boundary conditions and loading.

C. Analysis Procedure

For each material case, total deformation, equivalent (von Mises) stress, and equivalent elastic strain were extracted for the full assembly and for each individual link. Modal analysis, performed on the Aluminium configuration (identified as the strength-optimal material from the structural results), extracted the first five natural frequencies and mode shapes for both models. Harmonic analysis was subsequently conducted over a 0-200 Hz frequency sweep to obtain amplitude response in the X, Y, and Z directions and identify resonance peaks.

V. RESULTS AND DISCUSSION

A. Deformation

Table I and Table II summarize the maximum total deformation obtained for each link under each material for Model 1 and Model 2 respectively. Across both configurations, Aluminium consistently produced the lowest deformation (8.02 mm for Model 1 and 8.96 mm for Model 2 at the end effector), while S-GFRP produced the highest (50.79 mm and 57.84 mm respectively). This confirms that despite its higher elastic modulus, S-GFRP's lower stiffness-to-weight response under the applied load and boundary conditions results in greater flexure than the metallic option.

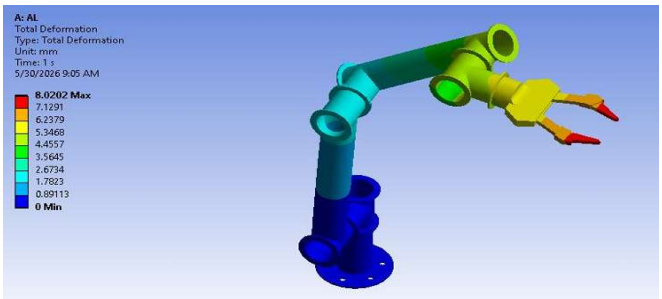


Fig 4: Maximum deformation on assembly.

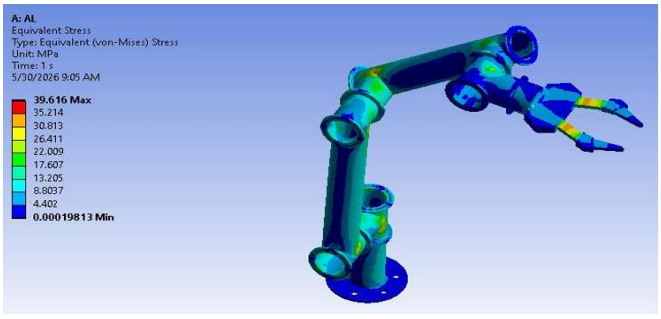


Fig 5: Bending stress of the robot structure.

International Journal Of Innovative Trends In Multi Disciplinary Scientific Research
ISSN (Online): 3139 – 2687
(www.ijtmsr.co.in) Volume 9, Issue 6, 2026

TABLE I. MAXIMUM DEFORMATION — MODEL 1 (mm)

Component	AL	CFRP	E-GFRP	S-GFRP
Robot structure	8.02	40.48	45.46	50.79
Link 1	0.066	0.456	0.44	0.55
Link 2	0.299	1.77	1.898	2.19
Link 3	2.5	14.49	15.61	17.84
Link 4	5.24	29.57	32.1	36.36
Link 5	5.6	31.33	34.16	38.59
Link 6	8.02	40.48	45.46	50.79

TABLE II. MAXIMUM DEFORMATION — MODEL 2 (mm)

Component	AL	CFRP	E-GFRP	S-GFRP
Robot structure	8.96	46.63	51.5	57.84
Link 1	0.066	0.456	0.44	0.551
Link 2	0.301	1.79	1.91	2.14
Link 3	2.73	16.2	17.24	19.79
Link 4	5.87	33.85	36.25	41.24
Link 5	6.29	35.93	38.66	43.86
Link 6	8.96	46.63	51.5	57.84

B. Bending (von Mises) Stress

Table III and Table IV present the equivalent von Mises stress results. The peak stress in both models occurs at Link 4 and at the overall assembly, coinciding with the connecting regions and sharp corners where stress concentration is expected. Aluminium exhibited the lowest peak stress (39.61 MPa in Model 1; 47.0 MPa in Model 2), whereas CFRP exhibited markedly higher stress concentrations (up to 136.4 MPa in Model 1), attributable to its higher stiffness redistributing load into a smaller effective cross-section under the same applied force.

TABLE III. BENDING STRESS — MODEL 1 (MPa)

Component	AL	CFRP	E-GFRP	S-GFRP
Robot structure	39.61	136.4	64.8	72.04
Link 1	14.59	13.14	13.53	13.25
Link 2	36.56	37.12	34.5	35.07
Link 3	38.84	45.76	34.6	33.28
Link 4	39.61	136.4	64.84	72.04
Link 5	30.12	59.11	38.04	40.51
Link 6	35.13	47.52	39.65	40.06

TABLE IV. BENDING STRESS — MODEL 2 (MPa)

Component	AL	CFRP	E-GFRP	S-GFRP
Robot structure	47.0	117.6	57.4	61.28
Link 1	14.64	13.16	13.55	13.32
Link 2	37.48	37.7	34.7	35.77
Link 3	45.52	52.8	44.31	44.42
Link 4	47.0	117.6	57.28	61.26
Link 5	30.47	58.8	38.15	40.57
Link 6	35.28	47.92	39.87	40.34

C. Strain and Mass Comparison

Equivalent elastic strain followed the same trend as stress and deformation, with Aluminium recording the minimum strain (0.00066) and S-GFRP the maximum (0.0054) at the critical Link 3/Link 6 locations. Table V compares the total assembly mass for each material across both models. Aluminium is the heaviest option (5.39-5.70 kg), while CFRP is the lightest (2.87-3.00 kg); however, this weight advantage is offset by CFRP's substantially higher stress and deformation response, indicating that mass reduction alone is an insufficient optimization criterion.

TABLE V. ASSEMBLY MASS COMPARISON

Material	Model 1 (kg)	Model 2 (kg)
Aluminium	5.39	5.70
CFRP	3.00	2.87
E-GFRP	3.89	3.73
S-GFRP	3.892	3.75

D. Modal and Harmonic Analysis

Modal analysis of the Aluminium structure (Table VI) shows that Model 1 possesses marginally higher natural frequencies than Model 2 across all five extracted modes, indicating slightly greater stiffness. The first natural frequency was 23.54 Hz for Model 1 versus 22.56 Hz for Model 2. Harmonic analysis over 0-200 Hz identified resonance peaks near the first bending mode (~23 Hz, Y-direction) and near the fourth mode (~82-88 Hz, Z-direction) for both models, indicating frequency ranges that should be avoided during operational actuation to prevent amplified vibration.

International Journal Of Innovative Trends In Multi Disciplinary Scientific Research
ISSN (Online): 3139 – 2687
(www.ijtmsr.co.in) Volume 9, Issue 6, 2026

TABLE VI. NATURAL FREQUENCY — ALUMINIUM STRUCTURE

Mode	Model 1 (Hz)	Model 2 (Hz)
1	23.54	22.56
2	27.79	23.61
3	81.95	78.22
4	87.61	82.28
5	193.33	185.37

E. Material and Model Selection

Considering all structural, modal, and harmonic results jointly, Aluminium is identified as the structurally optimum material: although it carries the highest mass among the four options, it produces the minimum deformation, stress, and strain in every link while remaining within allowable stress limits, and provides the highest structural stiffness (natural frequency). Between the two geometric configurations, Model 2 offers a reduced overall mass relative to Model 1 at the cost of marginally higher deformation and stress; since these increases remain within allowable limits, Model 2 is recommended as the preferred configuration where mass reduction is prioritized, while Model 1 remains preferable where maximum stiffness is the governing requirement.

VI. CONCLUSION

A comparative structural, modal, and harmonic FEA study was carried out on two link-geometry configurations of a 30 kg-payload logistics robotic arm using Aluminium, CFRP, E-GFRP, and S-GFRP. Aluminium consistently delivered the lowest deformation, stress, and strain across both configurations and all six links, establishing it as the preferred material despite its comparatively higher mass. Model 2 achieved a lower overall assembly mass than Model 1 while maintaining deformation and stress within allowable limits, making it the recommended geometric configuration. Modal analysis confirmed adequate separation between the identified natural frequencies and expected operating frequencies, while harmonic analysis highlighted specific frequency bands (near 23 Hz and 82-88 Hz) requiring avoidance during operation to prevent resonance. The proposed methodology offers a replicable framework for balancing weight, strength, and dynamic stability in the design of logistics material-handling robotic manipulators.

VII. FUTURE SCOPE

Future work may explore advanced materials such as carbon nanotube-reinforced or hybrid composites for further weight reduction; multi-physics and fluid-structure interaction simulations for more realistic operating-environment predictions; multi-objective design optimization algorithms balancing mass, stiffness, and cost simultaneously; and the development of adaptive control strategies to accommodate dynamic loading variability during real-world logistics operation. Physical prototyping and experimental validation of the FEA predictions would further strengthen confidence in the recommended Aluminium/Model 2 configuration.

REFERENCES

[1] R. Yazdanpanah, "Geometric Jacobians derivation and kinematic singularity analysis for Smokie robot manipulator and the Barrett WAM," in Proc. 5th Int. Conf. Robotics and Mechatronics (ICROM), 2017.

[2] J. A. Hansen, K. C. Gupta, and S. M. K. Kazerounian, "Generation and evaluation of the workspace of a manipulator," Int. J. Robotics Research, vol. 2, pp. 665-672, 1983.

[3] N. Mir-Nasiri, "Design, modelling and control of four-axis parallel robotic arm for assembly operations," Assembly Automation, vol. 24, no. 4, pp. 365-369, 2004.

[4] D. I. Park, C. Park, H. Do, T. Choi, and J. Kyung, "Design and analysis of dual arm robot using dynamic simulation," in Proc. 10th Int. Conf. Ubiquitous Robots and Ambient Intelligence (URAI), Jeju, Korea, 2013.

[5] R. J. Schilling, Fundamentals of Robotics: Analysis & Control. Upper Saddle River, NJ: Prentice Hall, 2011.

[6] T. C. Manjunath, "Kinematic modelling and maneuvering of a 5-axes articulated robot arm," World Acad. Sci. Eng. Technol., pp. 364-370, 2007.

[7] K. Kreutz-Delgado, M. Long, and H. Seraji, "Kinematic analysis of 7-DOF anthropomorphic arms," in Proc. IEEE Int. Conf. Robotics and Automation, 1990, pp. 824-830.

[8] J.-S. Oh, J.-D. Kim, and J.-H. Kwak, "Design of a control system for welding robot with tracking simulation," in Proc. Int. Welding/Joining Conf. Korea, 2007, pp. 251-258.

[9] J. Lloyd, "Kinematics of common industrial robots," Robotica, vol. 4, no. 2, pp. 169-191, 1988.

[10] P. Bhatia, J. Thirunarayanan, and N. Dave, "An expert system-based design of SCARA robot," Expert Systems with Applications, vol. 15, pp. 99-109, 1998.

[11] S. Clark and Y. J. Lin, "CAD tools integration for robot kinematics design assurance with case studies on PUMA robots," Industrial Robot, vol. 34, no. 3, pp. 240-248, 2007.

[12] D. Xu, C. A. Acosta Calderon, J. Q. Gan, H. Hu, and M. Tan, "An analysis of the inverse kinematics for a 5-DOF manipulator," Int. J. Automation and Computing, pp. 114-124, Feb. 2005.

[13] M. Vukobratovic, D. Potkonjak, and H. Inoue, "Dynamics and robust control of robot-environment interaction," World Scientific, 2002.

[14] D. G. Lee, C. S. Lee, H. G. Lee, H. Y. Hwang, and J. W. Kim, "Novel applications of composite structures to robots, machine tools and automobiles," Composite Structures, vol. 66, pp. 17-39, 2004.

[15] J. Lee, D. Y. Lee, J. Park, I. Choi, J. W. Lim, S. Kim, and D. G. Lee, "Carbon/epoxy composite foot structure for biped robots," Composite Structures, vol. 140, pp. 344-350, 2016.

[16] G. Pandey and Sreekumar M., "Development of high strength bio-composite material for light weight serial robot mechanisms," Int. J. Advance Research, Ideas and Innovations in Technology, 2015, pp. 512-521.

[17] H. Ku, H. Wang, N. Pattarachaiyakoop, and M. Trada, "A review on the tensile properties of natural fiber reinforced polymer composites," Composites Part B, vol. 42, pp. 856-873, 2011.

[18] H. Das, X. Bao, Y. Bar-Cohen, R. Bonitz, R. Lindemann, M. Maimone, I. Nesnas, and C. Voorhees, "Robot manipulator technologies for planetary exploration," in Proc. 6th Annu. Int. Symp. Smart Structures and Materials, Newport Beach, CA, 1999, paper 3668-17.

[19] K. S. Meenalochani and V. Reddy, "A review on water absorption behavior and its effect on mechanical properties of natural fibre reinforced composites," Int. J. Innovative Research in Advanced Engineering, vol. 4, no. 4, 2017.

[20] F. Gordaninejad and N. G. Chalhoub, "Dynamic analysis of a composite-material flexible robot arm," Computers & Structures, vol. 49, no. 2, pp. 315-327, 1993.

[21] F. Gordaninejad, "Active and passive control of a revolute-prismatic flexible composite-material robot arm," Computers & Structures, vol. 53, no. 4, pp. 867-875, 1994.

[22] K.-C. Hung, H. Yeh, and T.-C. Yang, "Characterization of wood-plastic composites made with different lignocellulosic materials that vary in their morphology, chemical composition and thermal stability," Polymers, vol. 9, p. 726, 2